

## Supplementary Materials for

### Comparative Phosphoproteomic Analysis of Checkpoint Recovery Identifies New Regulators of the DNA Damage Response

Vincentius A. Halim, Mónica Alvarez-Fernández, Yan Juan Xu, Melinda Aprelia, Henk W. P. van den Toorn, Albert J. R. Heck, Shabaz Mohammed, René H. Medema\*

\*Corresponding author. E-mail: r.medema@nki.nl

Published 23 April 2013, *Sci. Signal.* **6**, rs9 (2013)  
DOI: 10.1126/scisignal.2003664

#### This PDF file includes:

Fig. S1. Schematic of the checkpoint recovery assay.  
Fig. S2. In-depth proteomics data analysis.  
Fig. S3. Enrichment of candidates with particular functions.  
Fig. S4. Astrin affects the p53/MDM2 feedback loop.  
Legends for tables S1 to S8

#### Other Supplementary Material for this manuscript includes the following: (available at [www.sciencesignaling.org/cgi/content/full/6/272/rs9/DC1](http://www.sciencesignaling.org/cgi/content/full/6/272/rs9/DC1))

Table S1 (.pdf format). All quantified phosphopeptides.  
Table S2 (.pdf format). All identified peptides (unphosphorylated).  
Table S3 (.pdf format). All identified proteins.  
Table S4 (.pdf format). Comparing phosphosites that are phosphorylated by PLK1 and phosphosites of Polo box interactors.  
Table S5 (.pdf format). Protein with changes on phosphopeptide abundance (at least in two experiments).  
Table S6 (.pdf format). Comparing phosphosites that are phosphorylated by PLK1 during recovery and also phosphorylated with pSQ/TQ motif upon DNA damage.  
Table S7 (.pdf format). Primary siRNA screen to identify proteins involved in recovery and unperturbed mitotic entry control.  
Table S8 (.pdf format). Secondary screen for siRNA pool deconvolution.

## SUPPLEMENTAL FIGURE LEGENDS

**Fig. S1.** Schematic of the checkpoint recovery assay. (A) Timeline of treatments for the phosphoproteomic analysis of checkpoint recovery. (B) Cell cycle profiles of asynchronous, thymidine arrested, thymidine released, doxorubicin treated and caffeine treated U2OS cells, representing the cell cycle states corresponding with the steps shown in (A). Percentage of cells arrested in G2 is indicated. (C) Mitotic index of U2OS cells synchronized in G2 and treated with doxorubicin (1 hour, 1  $\mu$ M) was determined by pH3 staining and FACs analysis. As indicated in (A), caffeine was added 18 hours after doxorubicin was removed and cells were fixed at the indicated time points. (D) The percentage of residual mitotic cells in doxorubicin-treated U2OS cultures treated either with caffeine and PLK1 inhibitor [BI2536 (BI), 100 nM] simultaneously, or with inhibitor 4 hours after caffeine treatment. Mitotic index was determined by pH3 staining and FACs analysis after shaking to remove most cells in mitosis. DMSO-treated cells were used as controls. (N=2 independent experiments).

**Fig. S2.** In-depth proteomics data analysis. (A) Regulated phosphosites identified in the PLK1 inhibitor experiments were compared to phosphosites of PLK1's polo box domain (PBD-PLK1) interactors. (B) Major kinases responsible for those regulated phosphosites were predicted using NetworKIN. (C) The experiment of 2 hours BI2536 was repeated and both data sets were compared. The ratio of co-quantified phosphopeptides (that were decreased in abundance) was plotted and the correlation coefficient was calculated. (D) Representative phosphosites identified in our proteomics study (table S1) were verified by Western blot analysis. Actin was used as loading control.

**Fig. S3.** Enrichment of candidates with particular functions. **(A)** Most significant protein functions [ $-\log(\text{significance})$ ] of the differentially phosphorylated proteins were determined by Ingenuity software using the right-tailed Fischer's exact test [Threshold  $1.3 = -\log(P=0.05)$ ]. **(B)** Panther classification molecular function of the proteins shown to be differentially phosphorylated during recovery ( $>2$ -fold difference in phosphopeptide ratio in at least 2 experiments).

**Fig. S4.** Astrin affects the p53/MDM2 feedback loop. **(A)** qRT-PCR analysis of *SPAG5*, *p53*, and *MDM2* mRNA abundance in GAPDH and Astrin-depleted cells 8 hours after doxorubicin treatment (1 hour, 1  $\mu\text{M}$ ). Expression was normalized to *ACTB*. mRNA levels in GAPDH-deficient cells were set as 1. A representative result from  $n = 2$  independent experiments is shown. **(B)** Fold change in expression of *p53* and *MDM2* mRNA abundance at 0, 4, 8, 12 and 16 hours after damage (1  $\mu\text{M}$  doxorubicin, 1 hour) in GAPDH and Astrin-depleted cells. Expression was normalized to that of *ACTB*. mRNA abundance at 0 hours were set as 1. A representative result from  $n = 2$  independent experiments is shown. **(C)** Protein abundance of MDM2, p53, and CDK4 (loading control) was determined by Western blot analysis of G2-synchronized U2OS cells transfected with the pool of siRNAs targeting Astrin or GAPDH, treated with doxorubicin (1 hour, 1  $\mu\text{M}$ ) then cycloheximide (chx), MG132 (mg), or both after doxorubicin was removed. Cells were collected and lysed 6 hours later. A representative blot from  $n = 2$  independent experiments is shown.

Table S1. All quantified phosphopeptides

Table S2. All identified peptides (unphosphorylated)

Table S3. All identified proteins

Table S4. Comparing phosphosites that are phosphorylated by PLK1 and phosphosites of Polo box interactors

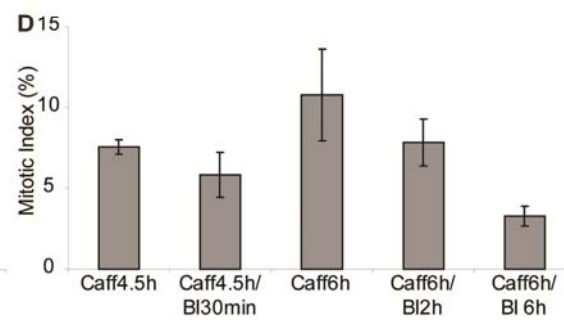
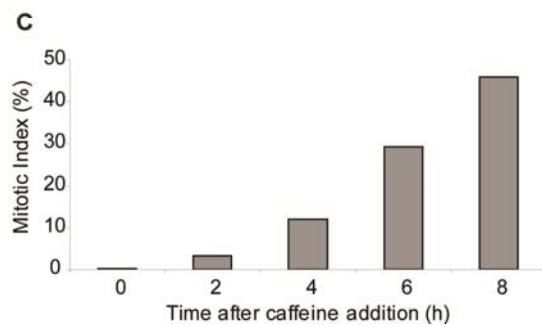
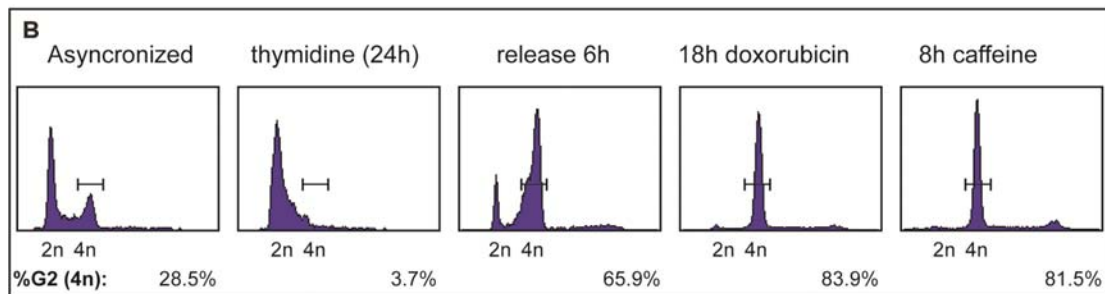
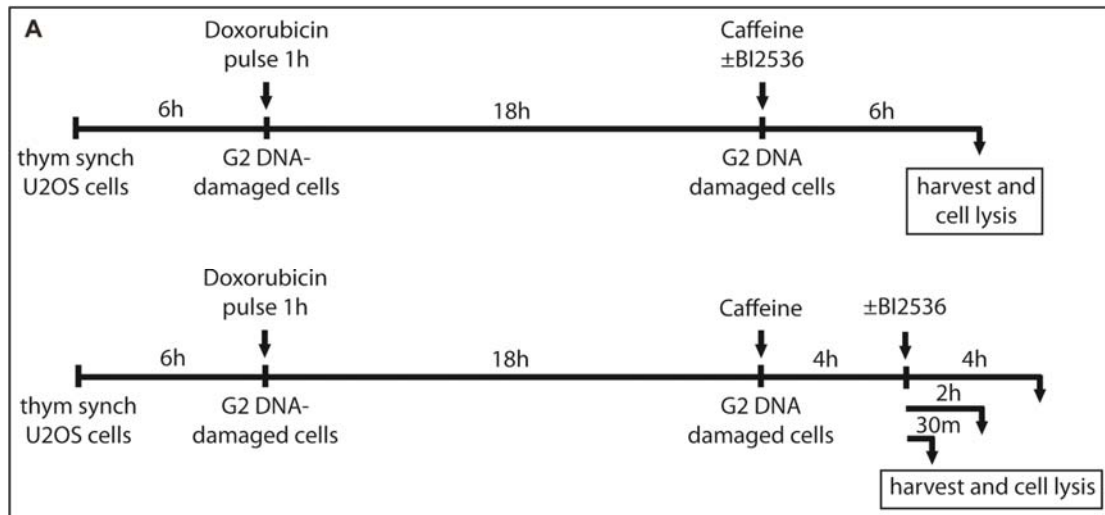
Table S5. Protein with changes on phosphopeptides abundance (at least in two experiments)

Table S6. Comparing phosphosites that are phosphorylated by PLK1 during recovery and also phosphorylated with pSQ/TQ motif upon DNA damage

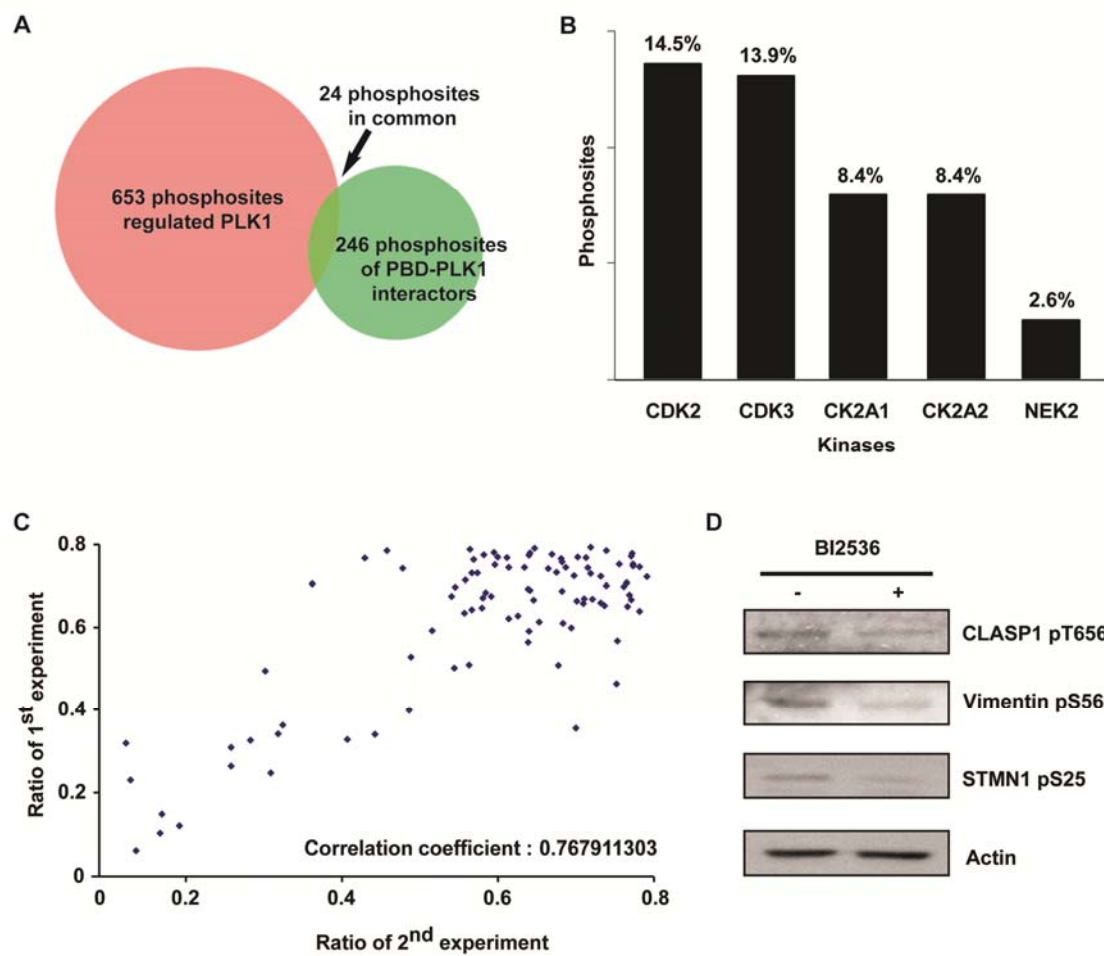
Table S7. Primary siRNA screen to identify proteins involved in recovery and unperturbed mitotic entry control

Table S8. Secondary screen for siRNA pool deconvolution

Suppl. Fig S1

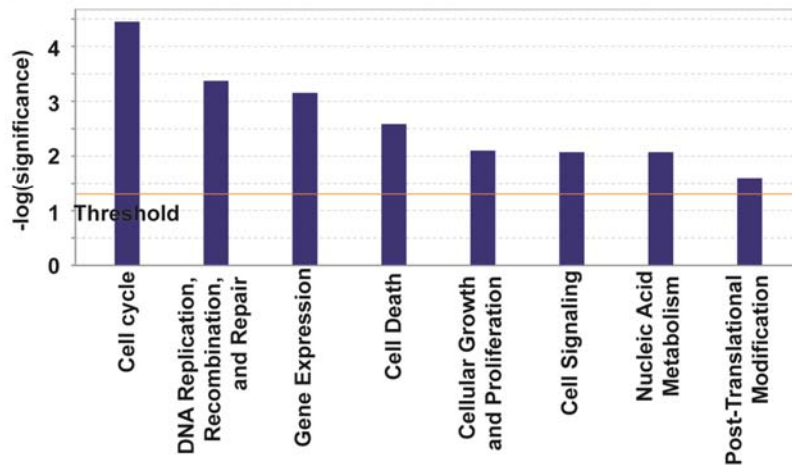


Suppl. Fig S2

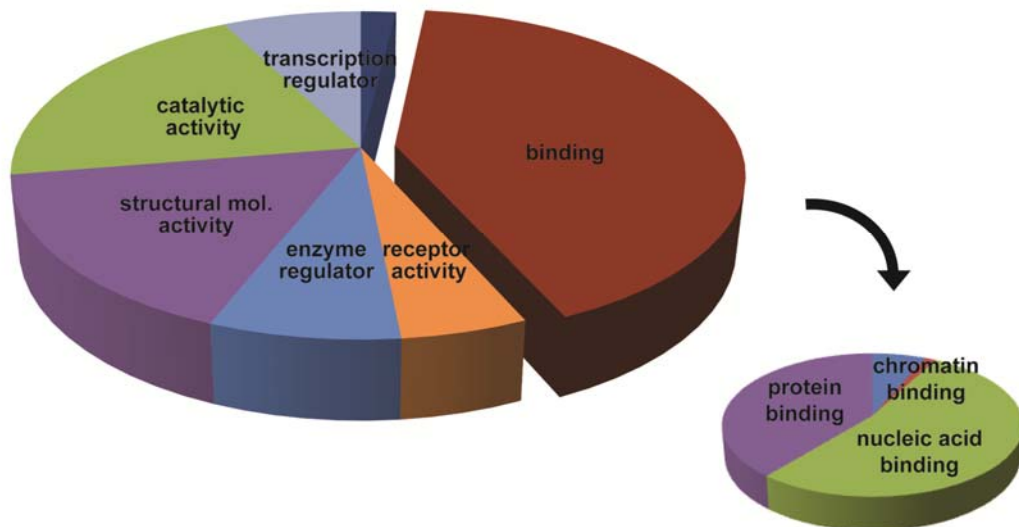


Suppl. Fig S3

A



B



Suppl. Fig S4

